



Published in final edited form as:

Mol Cancer Ther. 2013 December ; 12(12): 2697–2708. doi:10.1158/1535-7163.MCT-13-0500.

Targeting Plasminogen Activator Inhibitor-1 Inhibits Angiogenesis and Tumor Growth in a Human Cancer Xenograft Model

Evan Gomes-Giacoia¹, Makito Miyake¹, Steve Goodison^{1,2}, and Charles J. Rosser^{1,2}

¹Cancer Research Institute, MD Anderson Cancer Center

²Nonagen Bioscience Corp, Orlando, Florida

Abstract

Cancers of the urinary bladder result in aggressive and highly angiogenic tumors for which standard treatments have only limited success. Patients with advanced disease have a 5-year survival rate of less than 20%, and no new anticancer agent has been successfully introduced into the clinic armamentarium for the treatment of bladder cancer in more than 20 years. Investigations have identified plasminogen activator inhibitor-1 (PAI-1), a serine protease inhibitor, as being highly expressed in several malignancies, including bladder cancer, in which high expression is associated with a poor prognosis. In this study, we evaluated PAI-1 as a potential therapeutic target for bladder cancer. PAI-1 expression was manipulated in a panel of cell lines and functional inhibition was achieved using the small molecule tiplaxtinin. Reduction or inhibition of PAI-1 resulted in the reduction of cellular proliferation, cell adhesion, and colony formation, and the induction of apoptosis and anoikis *in vitro*. Treatment of T24 xenografts with tiplaxtinin resulted in inhibition of angiogenesis and induction of apoptosis, leading to a significant reduction in tumor growth. Similar results were obtained through evaluation of the human cervical cancer HeLa cell line, showing that PAI-1-mediated effects are not restricted to tumor cells of bladder origin. Collectively, these data show that targeting PAI-1 may be beneficial and support the notion that novel drugs such as tiplaxtinin could be investigated as anticancer agents.

© 2013 American Association for Cancer Research.

Corresponding Author: Charles J. Rosser, Cancer Research Institute, MD Anderson Cancer Center, 6900 Lake Nona Boulevard, Orlando, FL 32827., Phone: 407-266-7401; Fax: 407-266-7402; deacdoc@aol.com.

Note: Supplementary data for this article are available at Molecular Cancer Therapeutics Online (<http://mct.aacrjournals.org/>).

Disclosure of Potential Conflicts of Interest

S. Goodison has ownership interest (including patents) and C.J. Rosser is the president of Nonagen Bioscience Corp.

Authors' Contributions

Conception and design: E. Gomes-Giacoia, S. Goodison, C.J. Rosser

Development of methodology: E. Gomes-Giacoia, M. Miyake, C.J. Rosser

Acquisition of data (provided animals, acquired and managed patients, provided facilities, etc.): E. Gomes-Giacoia, M. Miyake

Analysis and interpretation of data (e.g., statistical analysis, biostatistics, computational analysis): E. Gomes-Giacoia, M. Miyake, C.J. Rosser

Writing, review, and/or revision of the manuscript: E. Gomes-Giacoia, S. Goodison, C.J. Rosser

Administrative, technical, or material support (i.e., reporting or organizing data, constructing databases): E. Gomes-Giacoia, S. Goodison, C.J. Rosser

Study supervision: S. Goodison, C.J. Rosser

Introduction

Cancer of the urinary bladder can be aggressive and develop resistance to currently available cancer therapies. An estimated 70,980 newly diagnosed cases of bladder cancer and 14,330 deaths from bladder cancer occurred in 2012 (1). When diagnosed as Ta/T1 lesion or even T2 lesion, cure with surgical resection is possible in a high percentage of cases, with a 5-year survival rate of more than 94% and 50%, respectively (2, 3). However, once metastatic disease develops, it is almost always fatal, with an estimated median survival of 12 to 14 months and a 5-year survival of more than 20% (4). The gold standard in the treatment of metastatic bladder cancer is the chemotherapeutic regimen of cisplatin and gemcitabine or methotrexate, vinblastine, adriamycin, and cisplatin (5, 6). Despite administration of these aggressive oncolytic cocktails, survival rates remain dismal (7), and no new anticancer agent has been successfully introduced into the clinic for the treatment of bladder cancer in more than 20 years. Thus, the identification of novel therapeutics against this disease is urgently required.

In bladder cancer biomarker discovery studies, we and others have previously identified plasminogen activator inhibitor-1 (PAI-1), also known as SERPINE1, as a molecule that is consistently overexpressed in bladder tumor cells (8–11). PAI-1 is an endogenous inhibitor of urokinase-type plasminogen activator (uPA), and its expression is regulated by a number of intrinsic factors (e.g., cytokines and growth factors) and extrinsic factors (e.g., cellular stress; ref. 12). Perturbation of PAI-1 and the uPA system has been shown to have both pro- and antitumoral effects in a number of cancer models, primarily by regulating migration, invasion, apoptosis, and angiogenesis (13–17). Thus, PAI-1 seems to play a pivotal role in tumor growth and may represent a potential therapeutic target for bladder cancer.

In this study, we manipulated the expression of PAI-1 in a panel of cell lines, and used tiplaxtinin (PAI-039), a small-molecule inhibitor of PAI-1 (18–20), to investigate the potential of PAI-1 as a therapeutic target. *In vitro*, silencing of PAI-1 was associated with an impedance of cellular and colony growth and cellular adhesion, and an induction of apoptosis. *In vivo*, reduced tumor cell PAI-1 was associated with dramatically reduced xenograft growth accompanied by an increase in apoptosis and a reduction in angiogenesis.

Materials and Methods

Cell culture and reagents

Human urothelial cell lines, T24 and UM-UC-14 [American Type Culture Collection (ATCC)], and UROtsa derived from benign bladder tissue (a generous gift from Dr. Donald Sens at the University of North Dakota School of Medicine, Grand Forks, ND) were used in this study. A human cervical cancer cell line, HeLa (ATCC), was available for confirmatory studies. Before use, short tandem repeat (STR) profiling of all cell lines was carried out by the Genetic Resources Core Facility (GRCF) at Johns Hopkins University. Cell lines were maintained in Dulbecco's Modified Eagle Medium (DMEM) or RPMI 1640 media as previously described (21). Primary human umbilical vein endothelial cells (HUVEC; Cambrex) were cultured in Endothelial Basal Medium -2 (EBM-2) basal media supplemented with the EGM-2 MV Kit (Lonza) containing 2% FBS. HUVEC cells of

passage 6 to 8 were used. All cells were maintained in a standard humidified incubator at 37°C in 5% CO₂. Tiplaxtinin (PAI-039), a small-molecule inhibitor of PAI-1, was purchased from Axon MedChem and dissolved in dimethyl sulfoxide at a stock concentration of 10 mmol/L and stored at -20°C.

Immunoblotting

Cell lysate and immunoblotting were previously described in ref. (22). Details and antibodies are listed in Supplementary Material.

Viability and colony formation assays

Briefly, cell lines, T24, UM-UC-14, UROtsa, and HeLa cells were plated in 96-well dishes in triplicate at 1×10^3 cells per well and allowed to adhere for 24 hours. Subsequently, tiplaxtinin was added to the wells and allowed to incubate at the indicated concentrations. Cellular proliferation was determined by CellTiter-Glo Luminescent Cell Viability Assay (Promega) according to manufacturer's instructions at 24 hours, and IC₅₀ of tiplaxtinin was determined in Graphpad Prism (GraphPad Software Inc.). Luminescence was measured using a FLUOstar OPTIMA Reader (BMG Labtech). Next, monolayer colony formation assay was performed as described previously (23). In short, 10^3 cells were plated into 6-well dishes and treated with and without tiplaxtinin at the indicated concentration for 72 hours. Culture media was aspirated, cells washed, and fresh complete media was added. Cells were incubated for an additional 14 days. After 14 days, colonies were fixed with 6.0% glutaraldehyde and stained with 0.5% crystal violet. The surviving fraction was calculated. For the soft agar colony formation assay, the Cell Biolabs CytoSelect 96-Well Cell Transformation Assay was used (Cell Biolabs Inc.). Briefly, 2×10^3 cells in 1:1:1 mixture of 1.2% agar solution, 2× DMEM/20% FBS media, and cell suspension were added to a 96-well flat-bottom microplate already containing a solidified base agar layer. Cells were incubated for 6 to 8 days at 37°C in 5% CO₂. Colony formation was quantified using the fluorescent cell stain CyQUANT GR Dye (Cell Biolabs Inc.) in the FLUOstar OPTIMA Reader. Examination of cell colony formation was also observed under a light microscope. At least three independent experiments consisting of each condition tested in triplicate wells were used to calculate mean ± SD values.

Gene transfection for stable cell lines

T24 and UM-UC-14 stable cells containing a functional null knockdown of PAI-1 (T24-PAI-1^{KD} clones 19 and 22 and UM-UC-14-PAI-1^{KD} clones 4 and 7) were generated using a plasmid with PAI-1 short hairpin RNA (shRNA) cloned within a pGFP-V-RS vector (Origene Technologies). A plasmid with a scrambled (Scr) non-effective shRNA construct in pGFP-V-RS was concomitantly produced as a negative control in each cell line (T24^{Scr} and UM-UC-14^{Scr}). HeLa stable cells overexpressing a functionally active PAI-1 (HeLa-PAI-1^{OE} 12 and 18) were produced using a plasmid containing a sequence-verified human PAI-1 cDNA cloned into a pCMV6-Entry vector. A plasmid with vector alone was transfected as an empty control (HeLa^{Empty}). T24 and UM-UC-14 stable cells were selected in medium containing 1 mg/mL of puromycin (Life Technologies) and HeLa stable cells were selected in medium containing 1,200 mg/mL of G418 (Life Technologies Inc.) for 14 days and subcloned by limiting dilution in 96-well plates. Integration of the transfected gene

into chromosome was confirmed by PCR. Stable cell lines were maintained in media containing 0.25 µg/mL of puromycin for T24 and UM-UC-14 clones and in media containing 500 µg/mL G418 for HeLa clones.

Quantitative reverse transcriptase PCR

RNA was extracted from cells using the RNeasy Mini Kit (Qiagen) as per the manufacturer's instructions. Conversion to cDNA was achieved through the High Capacity cDNA Reverse Transcription Kit (Life Technologies). Quantitative reverse transcriptase (RT) PCR was carried out using the ABI 7300 Real-Time PCR System (Life Technologies) in a 20-µL reaction volume containing 1 µL of the first-strand cDNA, 1 µmol/L of gene-specific TaqMan primer and probe mix (Hs01126606_m1; Applied Biosystems). Relative fold changes in mRNA levels were calculated after normalization to β-actin using the comparative C_t method (24).

Measurement of secreted PAI-1 by ELISA

Cells were plated onto 6-well plates at a density of 2×10^5 cells per well. After 48 hours, the conditioned media was collected and centrifuged to remove any dead or floating cells. Conditioned media was analyzed by ELISA assay for PAI-1 (Abcam) using a FLUOstar OPTIMA Reader (BMG Labtech). At least three independent experiments consisting of each condition tested in triplicate wells were used to calculate mean \pm SD values.

Zymography

Thirty micrograms of total cell lysate from the urothelial cell lines T24, UM-UC-14, and UROtsa, as well as the cervical cancer cell line HeLa treated in the presence and absence of tiplaxtinin at 10, 20, 30, 40, and 50 µmol/L and 30 µg of total cell lysate from the T24-PAI-1^{KD} 19 and 22 clones, T24^{Scr}, UM-UC-14-PAI-1^{KD} 4 and 17 clones, UM-UC-14^{Scr}, HeLa-PAI-1^{OE} 12 and 18 clones, and HeLa^{Empty}, were electrophoresed on 10% SDS-polyacrylamide gels containing 1 mg/mL casein (Sigma-Aldrich), 10 µg/mL plasminogen (Sigma-Aldrich), and 0.5 mU/mL uPA under nonreducing conditions. After electrophoresis and SDS removal, PAI-1 renaturation was achieved by washing the gel for 1 hour in buffer containing 2.5% Triton-X 100, 50 mmol/L Tris pH 7.4, 5 mmol/L CaCl₂, and 1 µmol/L ZnCl₂. Gels were then incubated in a reaction buffer containing 50 mmol/L Tris pH 7.4, 5 mmol/L CaCl₂, 1 µmol/L ZnCl₂, and 0.02% NaN₃ pH 8.0 for 18 hours at 37°C, followed by staining with Coomassie blue. PAI-1 activity was indicated as lytic zones of plasmin generation. Gels were photographed using the KODAK Gel Logic 200 Imaging System with Carestream Molecular Imaging Software Standard Edition v5.0.7.24 (Carestream Health).

Apoptosis and anoikis assays

Parental T24, UM-UC-14, UROtsa, and HeLa cells treated with or without tiplaxtinin, as well as the T24-PAI-1^{KD} 19 and 22 clones, T24^{Scr}, UM-UC-14-PAI-1^{KD} 4 and 17 clones, UM-UC-14^{Scr}, HeLa-PAI-1^{OE} 12 and 18 clones, and HeLa^{Empty}, were assessed in a LIVE/DEAD Annexin V apoptotic assay (BD Biosciences) by flow cytometry. Furthermore, resistance to apoptosis was also determined in parental T24, UM-UC-14, UROtsa, and HeLa cells treated with or without pretreatment of tiplaxtinin and in the above clones by exposure

in the presence and absence of 5 $\mu\text{g}/\text{mL}$ of mitomycin C (an agent capable of inducing apoptosis) for 48 hours. In brief, after 48 hours of exposure to mitomycin C, cells were trypsinized, washed with $1\times$ PBS, and stained with propidium iodide in tandem with an Allophycocyanin (APC)-conjugated annexin V antibody according to the manufacturer's instructions (BD Biosciences) and quantitated via flow cytometry using the BD FACSCalibur with CellQuest Pro Software (BD Biosciences) and FlowJo (TreeStar Inc.). Viable cells are negative for both annexin V and propidium iodide, early apoptotic cells exhibit externalization of phosphatidylserine and are annexin V-positive but have an intact plasma membrane and are propidium iodide negative, whereas dead and damaged cells that have subsequently lost their membrane integrity are positive for both annexin V and propidium iodide. For anoikis studies, parental T24, UM-UC-14, UROtsa, and HeLa cells pretreated with or without tiplaxtinin, as well as the T24, UM-UC-14, and HeLa clones, were plated in 24-well dishes precoated with poly-Hema preventing cell attachment to substratum. Cells were cultured for 24, 48, and 72 hours and were then assessed for cell viability using the CellTiter-Glo Luminescent Cell Viability Assay (Promega) according to the manufacturer's instructions. At least three independent experiments consisting of each condition tested in triplicate wells were used to calculate mean \pm SD values.

Adhesion assay

Ninety-six-well plates were precoated with 10 $\mu\text{g}/\text{mL}$ of collagen (Sigma-Aldrich) in PBS at 37°C for 1 hour. The wells were blocked with 0.5% bovine serum albumin (BSA) in culture medium and 0.1% BSA in medium was used as the washing buffer. Parental T24, UM-UC-14, UROtsa, and HeLa cells treated with or without tiplaxtinin, as well as the T24-PAI-1^{KD} 19 and 22 clones, T24^{Scr}, UM-UC-14-PAI-1^{KD} 4 and 17 clones, UM-UC-14^{Scr} HeLa-PAI-1^{OE} 12 and 18 clones, and HeLa^{Empty}, were serum-starved overnight, released from dishes via cell dissociation buffer (Life Technologies), and seeded at 10^4 cells per well in precoated white-walled 96-well plates. Cells were preincubated with tiplaxtinin for 1 hour before detachment. After release from tissue culture dishes, cells were rinsed with PBS and resuspended in serum-free medium containing the appropriate concentration of inhibitors. Cells were washed twice with PBS at 30, 60, and 120 minutes. At each time point, nonadherent cells were removed by washing, and adherent cells were quantified using CellTiter-Glo Luminescent Cell Viability Assay as described earlier. At least three independent experiments consisting of each condition tested in triplicate wells were used to calculate mean \pm SD values.

Endothelial cell tube formation assays

Matrigel (BD Biosciences) was added to 96-well plates (40 $\mu\text{L}/\text{well}$) and allowed to solidify for 30 minutes at 37°C . HUVEC cells were seeded on top of Matrigel in triplicates at a density of 10^4 cells per well in EBM-2 basal media with or without 250 ng/mL of recombinant PAI-1 (Peprotech) and with or without tiplaxtinin before seeding on top of Matrigel and incubated for 6 hours. In addition, HUVEC cells were seeded on top of Matrigel in triplicates at a density of 1×10^4 cells per well in conditioned media from cultured T24-PAI-1^{KD} 19 and 22 clones, T24^{Scr}, UM-UC-14-PAI-1^{KD} 4 and 17 clones, UM-UC-14^{Scr}, HeLa-PAI-1^{OE} 12 and 18 clones, and HeLa^{Empty} and allowed to incubate for 6 hours. Images of capillary tube formation were captured using Leica DMIL inverted

microscopy at 6 hours after seeding. The angiogenic activities were quantitatively evaluated by measuring the total tube length of capillary tube in at least four viewed fields per well. At least three independent experiments consisting of each condition tested in triplicate wells were used to calculate mean \pm SD values.

***In vivo* administration of PAI-1 inhibitor**

The importance of PAI-1 expression for tumorigenicity was assessed in an *in vivo* bladder cancer and cervical cancer mouse models. Animal care was in compliance with the recommendations of the Guide for Care and Use of Laboratory Animals (National Research Council) and approved by our local Institutional Animal Care and Use Committee (IACUC). The subcutaneous tumorigenicity assay was performed in athymic BALB/c nu/nu mice (6 to 8 weeks old) purchased from Harlan Laboratories by inoculating 2×10^6 parental T24 cells and 2×10^6 parental HeLa cells as described previously (22, 25). After 2 weeks, mice bearing bladder xenografts and mice bearing cervical xenografts were divided randomly into three groups (control, 5 mg/kg of tiplaxtinin, and 20 mg/kg of tiplaxtinin) and treatment was initiated. Each group was composed of at least 10 mice. No toxicity or weight loss was noted in any of the treatment groups. Tiplaxtinin (100 μ L diluted in corn oil) was administered via oral gavage daily (Monday–Friday) for 5 weeks. Control mice received vehicle alone on the same schedule. Tumor volumes were measured weekly with digital calipers and calculated by $V (\text{mm}^3) = \text{length} \times (\text{width})^2 \times 0.5236$. After 5 weeks, the mice were sacrificed, tumors resected, and analyzed by immunohistochemical staining.

Immunohistochemical analysis of xenograft tumors

Immunohistochemistry was conducted as described in refs. (22, 25). Details and antibodies are listed in Supplementary Material.

Statistical analyses

All experimental data were expressed as mean with standard deviation. All statistical analyses were conducted using a Student *t* test, Mann–Whitney nonparametric *U* test, or one-way ANOVA and compared with the controls. A *P* value less than 0.05 was considered significant. All statistical analyses and figures were carried out using GraphPad Prism software 5.0 (GraphPad Software Inc.).

Results

Inhibition of cellular proliferation and colony formation by a small-molecule inhibitor of PAI-1

The expression of PAI-1 was evaluated in a panel of human bladder cell lines (Fig. 1A): UROtsa (benign bladder), T24 (high-grade urothelial cancer), and UM-UC-14 (low-grade urothelial cancer). Western blot analysis, quantitative PCR, and ELISA data revealed significantly elevated levels of PAI-1 in T24 and UM-UC-14 cells compared with UROtsa (Fig. 1A). Next, we examined the effects of tiplaxtinin [1-benzyl-5-[4-(trifluoromethoxy)phenyl]-1H-indol-3-yl] (oxo) acetic acid, PAI-039], a small-molecule inhibitor of PAI-1 activity (18), on the urothelial cell lines. The role of PAI-1 in malignant cell growth and colony outgrowth was confirmed by a proliferation assay in which urothelial cells were

treated with increasing concentrations of tiplaxtinin at predetermined time intervals. A significant inhibition in cellular proliferation was noted in T24 cells treated with tiplaxtinin with the documentation of a favorable IC_{50} value of $43.7 \pm 6.3 \mu\text{mol/L}$ and in UM-UC-14 cells $52.8 \pm 1.6 \mu\text{mol/L}$ whereas the benign cell line, UROtsa, was noted to have a higher IC_{50} value of $70.3 \pm 0.1 \mu\text{mol/L}$ (data not shown).

Moreover, PAI-1 expression has been shown to enhance the clonal growth of cells (26, 27). Therefore, we investigated whether silencing of PAI-1 with tiplaxtinin would affect colony growth by performing both monolayer colony formation and soft agar assays. After 14 days there was complete inhibition of colony formation in T24 ($P < 0.0001$) and UM-UC-14 ($P < 0.0001$) cells treated with $50 \mu\text{mol/L}$ tiplaxtinin compared with UROtsa that showed only a 36% reduction in colony growth at $50 \mu\text{mol/L}$ ($P = 0.3912$; Fig. 1B). Confirmation of this clonal inhibition was documented in a soft agar assay. After 6 to 8 days, there was a 57% ($P < 0.0001$), 47% ($P = 0.0016$) and 13% ($P = 0.4489$) inhibition in colony formation in T24, UM-UC-14, and UROtsa cells, respectively, treated with tiplaxtinin at $50 \mu\text{mol/L}$ compared with their control counterparts (Fig. 1C).

Similarly, stable knockdown of PAI-1 in T24 and UC-UM-14 cells using shRNA transfection also resulted in a significant inhibition of colony formation in both the clonogenic and soft agar assays. We created stable knockdown clones of PAI-1 in the urothelial cells T24 (2 clones; T24-PAI-1^{KD}-19 and T24-PAI-1^{KD}-22) and UM-UC-14 (2 clones; UM-UC-14-PAI-1^{KD}-4 and UM-UC-14-PAI-1^{KD}-17). We also created PAI-1 high-expressor clones of the cervical tumor cell line HeLa (HeLa-PAI-1^{OE}-12 and HeLa-PAI-1^{OE}-18). These stable transfectants were compared with scrambled or empty vector transfectant controls (T24^{Scr}, UM-UC-14^{Scr}, and HeLa^{Empty}) in a panel of *in vitro* assays. Altered PAI-1 expression in stable transfectants was confirmed at the mRNA, protein, and secreted protein levels (Supplementary Fig. S1A–C). Reduction in PAI-1 expression by genetic manipulation and by tiplaxtinin was confirmed with a zymogen activity assay for PAI-1. An increase in the conversion of plasminogen to plasmin reflects a functional decrease in PAI-1 activity (Supplementary Fig. S1D).

In clonogenic assays, stable knockdown PAI-1 clones had a reduction of 39% ($P = 0.0037$) in T24-PAI-1^{KD}-19, 52% ($P = 0.0224$) in T24-PAI-1^{KD}-22, 37% ($P = 0.0003$) in UM-UC-14-PAI-1^{KD}-4, and 54% ($P = 0.0055$) in UM-UC-14-PAI-1^{KD}-17 cells (Supplementary Fig. S2A). In soft agar assays, reductions were observed at 55% ($P = 0.0011$) in T24-PAI-1^{KD}-19, 48% ($P = 0.0027$) in T24-PAI-1^{KD}-22, 29% ($P = 0.0014$) in UM-UC-14-PAI-1^{KD}-4, and 18% ($P = 0.0001$) in UM-UC-14-PAI-1^{KD}-17 (Supplementary Fig. S2B) compared with their respective controls. HeLa cells behaved similarly to the bladder cell lines. At $50 \mu\text{mol/L}$ tiplaxtinin, colony formation was completely inhibited in both the clonogenic assay (Supplementary Fig. S3A) and the soft agar assay (Supplementary Fig. S3B). Together, these data indicate that PAI-1 plays an integral role in cellular growth of human cancer cells.

PAI-1 influences apoptosis and anoikis

To determine if PAI-1 played a role in apoptosis, we investigated whether treatment with tiplaxtinin in T24, UM-UC-14, and UROtsa, and genetic manipulation of PAI-1 in T24 and

UM-UC-14 cells, would influence apoptosis in two independent assays. We assessed whether PAI-1 depletion influenced apoptosis in the presence and absence of the apoptotic agent, mitomycin C. In flow cytometric assays, the apoptotic fractions were increased in the PAI-1-depleted T24 clones, T24-PAI-1^{KD}-19 and T24-PAI-1^{KD}-22, by 26% ($P < 0.0001$) and 18% ($P < 0.0001$), respectively, compared with control T24^{Scr}, and in the UM-UC-14 clones, UM-UC-14-PAI-1^{KD}-4 and UM-UC-14-PAI-1^{KD}-17, by 13% ($P = 0.0003$) and 10% ($P = 0.0029$), respectively, compared with control UM-UC-14^{Scr}. Mitomycin C treatment (5 $\mu\text{g}/\text{mL}$) of T24^{Scr} alone induced a 10% increase in apoptosis over nontreated T24^{Scr} control, and this effect was further increased in the PAI-1-depleted clones, T24-PAI-1^{KD}-19 by 33% ($P < 0.0001$) and T24-PAI-1^{KD}-22 by 18% ($P = 0.0019$; Fig. 2A). In UM-UC-14 clones treated with mitomycin C, increased rates of apoptosis were noted in UM-UC-14-PAI-1^{KD}-4 (26%, $P = 0.0079$) and UM-UC-14-PAI-1^{KD}-17 (23%, $P = 0.0134$), whereas mitomycin treatment alone only showed an increase of 5% ($P = 0.0236$) over untreated control cells (Fig. 2A). Furthermore, parental T24 cells treated with tiplaxtinin showed an increase of 18% in apoptotic activity at 50 $\mu\text{mol}/\text{L}$ compared with non-treated control ($P < 0.0001$). When mitomycin C was added to tiplaxtinin in this system, 51% ($P < 0.0001$) of T24 cells were noted to undergo apoptosis, a significant increase over tiplaxtinin alone (18%; $P < 0.0001$) or apoptotic-inducing agent alone (22%, $P < 0.0001$; Fig. 2B). Furthermore, parental UM-UC-14 cells treated with tiplaxtinin showed an increase in apoptotic activity of 12% at 50 $\mu\text{mol}/\text{L}$ compared with nontreated control ($P < 0.0001$). When mitomycin C was added to tiplaxtinin, 28% ($P = 0.0022$) of UM-UC-14 cells were noted to undergo apoptosis, a significant increase over tiplaxtinin alone (12%, $P < 0.0001$) or apoptotic-inducing agent alone (15%, $P = 0.0001$; Fig. 2B). Interestingly, treatment of benign UROtsa cells with tiplaxtinin showed no significant alteration in apoptosis ($P = 0.2877$; Fig. 2B). In addition, as confirmed by Western blot analysis, tiplaxtinin induced both activation of caspase-3 and cleavage of PARP in all cell lines, whereas no change was evident in treated UROtsa cells (Fig. 2C). Western blot analysis data also revealed that apoptosis in the malignant bladder cell lines was mediated by the activation of Fas and FasL (Fig. 2C). Similarly, treatment of HeLa cells with tiplaxtinin resulted in increased rates of programmed cell death and the effect of mitomycin C was enhanced relative to PAI-1 expression (Supplementary Fig. S4). Our results indicate that reducing PAI-1 activity, either by genetic manipulation or by treatment with tiplaxtinin, induces cancer cell death.

Previous studies have shown that cell adhesion is associated with vulnerability to apoptosis (28, 29). Here, we confirmed that the suppression of PAI-1 resulted in a significant dose-response reduction in cellular adhesion in parental T24, UM-UC-14, and UROtsa cells after pretreatment with tiplaxtinin for 30 minutes (Fig. 3A). To further expand on our *in vitro* apoptosis data, we evaluated whether tiplaxtinin could induce anoikis (programmed cell death of detached cells). Cells were detached and cultured in suspension, and cell viability was monitored at 24, 48, and 72 hours. All cell lines (T24, UM-UC-14, and UROtsa) treated with tiplaxtinin exhibited similar reductions in viability of detached cells, supporting PAI-1 as a vital factor for normal cell physiology (Fig. 3B). Notably, IC_{50} values of tiplaxtinin in detached cells, $19.7 \pm 3.8 \mu\text{mol}/\text{L}$ in T24, $44.5 \pm 6.5 \mu\text{mol}/\text{L}$ in UM-UC-14, and $31.6 \pm 6.1 \mu\text{mol}/\text{L}$ in UROtsa, were significantly lower than the IC_{50} values calculated for cells cultured in the presence of tiplaxtinin under attached conditions ($43.7 \pm 6.3 \mu\text{mol}/\text{L}$ in T24,

52.8 ± 1.6 μmol/L in UM-UC-14, and 70.3 ± 0.1 μmol/L in UROtsa). Knockdown of PAI-1 in T24 and UC-UM-14 clones also resulted in a marked inhibition of cellular growth of cells in a detached state (Fig. 3B). Consistent with the above results, HeLa cells treated with tiplaxtinin were noted to have a reduction in the ability to attach and an induction in cell death in detached cells (Supplementary Fig. S4D and E). However, the IC₅₀ value for tiplaxtinin-treated HeLa cells under detached conditions (29.3 ± 2.2 μmol/L) was not lower than cells attached to a substratum (25.6 ± 1.8 μmol/L). Collectively, these data indicate that the ability of cells to adhere and detachment-induced cell death may be modulated by targeting PAI-1.

Endothelial tube formation is influenced by soluble PAI-1

It is reported that PAI-1 can play a key role in angiogenesis (30, 31). The significance of PAI-1 expression in cellular angiogenic potential was confirmed by performing tube formation assays in which HUVEC cells were cultured in growth factor-rich Matrigel with/without tiplaxtinin and/or recombinant PAI-1 (rhPAI-1). The total length of tube-like structures formed by HUVECs in the assay was significantly enhanced with the addition of 100 ng/mL of rhPAI-1 compared with control (20%; $P < 0.0001$), whereas total length of tube-like structures was significantly reduced upon the subsequent addition of 30 μmol/L tiplaxtinin (44%; $P < 0.0001$) and to an even greater extent with the addition of 50 μmol/L tiplaxtinin (68%; $P < 0.0001$; Fig. 4A). Conditioned media from the T24-PAI-1^{KD}, T24^{Scr}, UM-UC-14-PAI-1^{KD}, and UM-UC-14^{Scr} clones were analyzed in the tube formation assay. The total length of tube-like structures in HUVECs was reduced compared with control conditioned media from T24-PAI-1^{KD}-19 (57%; $P < 0.0001$), T24-PAI-1^{KD}-22 (53%; $P < 0.0001$), UM-UC-14-PAI-1^{KD}-4 (45%; $P < 0.0001$), and UM-UC-14-PAI-1^{KD}-17 (23%; $P < 0.0001$; Fig. 4B). Thus, PAI-1 may be a valid antiangiogenesis therapeutic target.

PAI-1 inhibition reduces tumor xenograft growth

Tiplaxtinin was administered by oral gavage to athymic mice bearing human bladder cancer cell line T24 xenografts and human cervical cancer HeLa cell xenografts. The subcutaneous tumor growth of both T24 and HeLa cell xenografts treated with tiplaxtinin was markedly reduced compared with untreated controls. Specifically, at the end of the study, control T24 xenografts were noted to be 1,150 ± 302 mm³ compared with 593 ± 328 mm³ for T24 xenograft tumors treated with 5 mg/kg tiplaxtinin ($P < 0.0001$) and 627 ± 248 mm³ for T24 xenografts treated with 20 mg/kg ($P < 0.0001$; Fig. 5A). Control HeLa xenografts were noted to be 1,159 ± 286 mm³ compared with 463 ± 198 mm³ for HeLa xenograft tumors treated with 5 mg/kg ($P < 0.0001$) and 474 ± 259 mm³ treated with 20 mg/kg ($P < 0.0001$; Supplementary Fig. S5A). A reduction in tumor PAI-1 was evident in tiplaxtinin-treated T24 (Fig. 5B) and HeLa (Supplementary Fig. S5B) xenografts by immunohistochemical staining. Expression levels of angiogenic marker CD31, proliferative index marker Ki-67, and apoptotic marker caspase-3 were also investigated in xenografts. Microvessel density (MVD) was calculated from CD31 staining for the 5 and 20 mg/kg treatment groups and a reduction in MVD by 69% ($P = 0.0008$) and 82% ($P < 0.0001$), respectively, compared with control was noted in T24 xenograft tumors (Fig. 5C). A reduction in MVD by 63% ($P = 0.0085$) and 85% ($P = 0.0018$), respectively, was noted in HeLa xenograft tumors (Supplementary Fig. S5C). Using Ki-67 immunostaining, the proliferative index was

calculated for the 5 and 20 mg/kg treatment groups and a reduction in the proliferative index by 53% ($P = 0.0156$) and 74% ($P = 0.0021$), respectively, compared with control was noted in T24 xenograft tumors (Fig. 5C). A reduction in the proliferative index by 53% ($P = 0.0192$) and 87% ($P < 0.0001$), respectively, compared with control was noted in HeLa tumors (Supplementary Fig. S5C). Finally, using caspase-3 immunostaining, an apoptotic index was calculated, and an enhancement in the apoptotic index by 1,069% ($P = 0.0172$) and 1,178% ($P = 0.0056$), for the 5 and 20 mg/kg treatment groups respectively, was observed in T24 xenograft tumors (Fig. 5C). Enhancements in the apoptotic index by 113% ($P = 0.1766$) and 823% ($P < 0.0001$), respectively, were observed in HeLa xenograft tumors (Supplementary Fig. S5C). Tiplaxtinin treatment of xenograft-bearing mice was associated with a reduction in tumor angiogenesis, a reduction in cellular proliferation, and an increase in apoptosis. These *in vivo* observations corroborate the *in vitro* findings, confirming that reduction of tumor cell PAI-1 expression can significantly impact tumor cell survival and that tiplaxtinin is a potentially potent antitumoral agent.

Discussion

PAI-1 is the primary inhibitor of tissue-type plasminogen activator (tPA) and uPA, and acts to suppress tissue and plasma fibrinolysis via plasmin conversion (32). PAI-1 is known to play a major role in benign disorders such as deep vein thrombosis, myocardial infarction, atherosclerosis, and stroke (33), and more recently has been linked to some cancers (19, 34). PAI-1 has been pursued as a target for drug development using tiplaxtinin, the second in a series of orally active PAI-1 inhibitors, with favorable pharmacokinetic and pharmacodynamic studies in large animals (35). However, to date, this is the first therapeutic study using tiplaxtinin in a cancer xenograft model.

In this study, we examined the tumorigenic and angiogenic effects of PAI-1 on human urothelial and cervical cell lines by genetically altering expression of PAI-1 and blocking PAI-1 with the small-molecule inhibitor tiplaxtinin. In contrast with the benign cell line UROtsa, the viability and growth of malignant T24, UM-UC-14, and HeLa cells were inhibited by PAI-1 reduction. Previous studies have linked PAI-1 effects on cellular proliferation to p53 (36). A p53 binding site is present within the PAI-1 gene promoter and is responsible for the stimulation of PAI-1 transcription. Cells that harbor mutant p53 have a reduction in PAI-1 promoter activity (36). Although HeLa cells possess wild-type p53, the T24 cell line is known to contain a novel p53 mutant that has an in-frame deletion of tyrosine 126. This p53 mutant is expressed at low levels, comparable with cell lines containing wild-type p53 alleles (37). Conversely, p53 is silenced in UROtsa cells by the binding of SV40 large T antigen, which may partially explain why UROtsa cells treated with tiplaxtinin did not undergo apoptosis as the other cells did. Furthermore, PAI-1 is expressed in a cell cycle-dependent manner with increased expression during growth activation (38). Thus, it is feasible that the novel p53 mutant in T24 still possesses the ability to bind to the PAI-1 promoter, leading to increased cellular proliferation.

The role of PAI-1 in tumor angiogenesis is controversial, with both promoting and inhibitory contributions described in previous studies (16, 17, 19, 30, 31, 34, 36, 39–44). These conflicting reports may be due to differences in tumor models, anatomic differences,

differences in the source of the PAI-1 (tumor cells vs. host cells), or due to expression levels of PAI-1 as well as PAI-2 and PAI-3. Despite this controversy, we demonstrated convincing data that (i) targeting PAI-1 in an *in vitro* assay significantly reduces cellular proliferation, cell adhesion, and colony formation, and induces apoptosis and anoikis and (ii) inhibition of PAI-1 by the administration of tiplaxtinin in T24 and HeLa xenografts reduced tumor growth by approximately 50% in both treated groups (5 and 20 mg/kg), which in turn was associated with a reduction in MVD and proliferative index and an increase in apoptosis.

Previous reports have demonstrated that the addition of PAI-1 to culture medium inhibited tumor cells from undergoing apoptosis (43). Interestingly, PAI-1 regulates apoptosis in transformed cells, but not in normal cells, suggesting a differential impact of PAI-1 between transformed and nontransformed cells (44). In this study, apoptotic assays were conducted with mitomycin C, an agent widely used in the intravesical treatment of non-muscle invasive bladder cancer (2). The addition of tiplaxtinin to mitomycin C potentiated the apoptotic effects seen with mitomycin C alone. Furthermore, on the basis of previous reports (45, 46), it stands to reason that systemic tiplaxtinin therapy could limit metastatic spread of tumors by inducing anoikis in detached cancer cells that have made their way to the extracellular matrix and vasculature. This programmed cell death is largely attributed to plasmin cleavage and activating FasL, a type-II transmembrane protein that belongs to the TNF family, whose activation induces apoptosis (ref. 47; Fig. 2C).

Little attention has been given to PAI-1 in human bladder or cervical tumors. For example, only three groups have reported on PAI-1 levels in human patients with bladder cancer. Urquidi and colleagues noted a significant increase in urothelial cell PAI-1 level (8) and urinary PAI-1 level (9) in patients bearing bladder tumors compared with non-tumor bearing patients. Another group noted increased expression of uPA, but not of PAI-1 expression, in a small cohort of patients with muscle invasive bladder cancer compared with nonmuscle invasive bladder cancer (48), and Becker and colleagues reported significantly higher PAI-1 levels in tissue and plasma samples, but not in urine, from patients with bladder cancer compared with controls (11). In cervical cancer, the literature on PAI-1 is scant. Kobayashi and colleagues demonstrated a significantly higher lymph node-positive rate in patients that had cervical tumors with strong uPA and/or PAI-1 tissue staining than in those with tumors with weak expression (49). In another study, Tee and colleagues noted a specific PAI-1 allelic polymorphism in women with cervical cancer compared with women without cervical cancer (50). Thus, further exploration of PAI-1 in human tumors is warranted.

Taken together, the results presented here show the importance in the expression of PAI-1 as it relates to tumor cell survival and tumor progression through angiogenesis. Reduction in xenograft growth with tiplaxtinin was accompanied with favorable alterations in angiogenesis, apoptosis, and cellular proliferation rates. Although PAI-1 function is complex, further investigation can exploit previous findings and determine whether small-molecule inhibitors of PAI-1 represent valid therapeutic agents for a variety of solid tumors.

Supplementary Material

Refer to Web version on PubMed Central for supplementary material.

Acknowledgments

Grant Support

This work was supported by the James and Esther King Biomedical Team Science Project 1KT-01 (to C.J. Rosser).

References

1. Siegel R, Naishadham D, Jemal A. Cancer statistics, 2013. *CA Cancer J Clin*. 2013; 63:11–30. [PubMed: 23335087]
2. Brausi M, Witjes JA, Lamm D, Persad R, Palou J, Colombel M, et al. A review of current guidelines and best practice recommendations for the management of nonmuscle invasive bladder cancer by the International Bladder Cancer Group. *J Urol*. 2011; 186:2158–67. [PubMed: 22014799]
3. Stenzl A, Cowan NC, De Santis M, Kuczyk MA, Merseburger AS, Ribal MJ, et al. Treatment of muscle-invasive and metastatic bladder cancer: update of the EAU guidelines. *Eur Urol*. 2011; 59:1009–18. [PubMed: 21454009]
4. Calabro F, Sternberg CN. Metastatic bladder cancer: anything new? 3. *Curr Opin Support Palliat Care*. 2012; 6:304–9. [PubMed: 22643704]
5. von der Maase H, Hansen SW, Roberts JT, Dogliotti L, Oliver T, Moore MJ, et al. Gemcitabine and cisplatin versus methotrexate, vinblastine, doxorubicin, and cisplatin in advanced or metastatic bladder cancer: results of a large, randomized, multinational, multicenter, phase III study. *J Clin Oncol*. 2000; 18:3068–77. [PubMed: 11001674]
6. von der Maase H, Sengelov L, Roberts JT, Ricci S, Dogliotti L, Oliver T, et al. Long-term survival results of a randomized trial comparing gemcitabine plus cisplatin, with methotrexate, vinblastine, doxorubicin, plus cisplatin in patients with bladder cancer. *J Clin Oncol*. 2005; 23:4602–8. [PubMed: 16034041]
7. Sternberg CN, de Mulder PH, Schornagel JH, Théodore C, Fossa SD, van Oosterom AT, et al. Randomized phase III trial of high-dose-intensity methotrexate, vinblastine, doxorubicin, and cisplatin (MVAC) chemotherapy and recombinant human granulocyte colony-stimulating factor versus classic MVAC in advanced urothelial tract tumors: European Organization for Research and Treatment of Cancer Protocol no 30924. *J Clin Oncol*. 2001; 19:2638–46. [PubMed: 11352955]
8. Urquidi V, Goodison S, Cai Y, Sun Y, Rosser CJ. A candidate molecular biomarker panel for the detection of bladder cancer. *Cancer Epidemiol Biomarkers Prev*. 2012; 21:2149–58. [PubMed: 23097579]
9. Goodison S, Chang M, Dai Y, Urquidi V, Rosser CJ. A multi-analyte assay for the non-invasive detection of bladder cancer. *PLoS ONE*. 2012; 7:e47469. [PubMed: 23094052]
10. Villadsen SB, Bramsen JB, Ostenfeld MS, Wiklund ED, Fristrup N, Gao S, et al. The miR-143/-145 cluster regulates plasminogen activator inhibitor-1 in bladder cancer. *Br J Cancer*. 2012; 106:366–74. [PubMed: 22108519]
11. Becker M, Szarvas T, Wittschier M, vom Dorp F, Totsch M, Schmid KW, et al. Prognostic impact of plasminogen activator inhibitor type 1 expression in bladder cancer. *Cancer*. 2010; 116:4502–12. [PubMed: 20564745]
12. Pyke C, Kristensen P, Ralfkiaer E, Eriksen J, Danø K. The plasminogen activation system in human colon cancer: messenger RNA for the inhibitor PAI-1 is located in endothelial cells in the tumor stroma. *Cancer Res*. 1991; 51:4067–71. [PubMed: 1855221]
13. Almholt K, Lund LR, Rygaard J, Nielsen BS, Danø K, Rømer J, et al. Reduced metastasis of transgenic mammary cancer in urokinase-deficient mice. *Int J Cancer*. 2005; 113:525–32. [PubMed: 15472905]
14. Shapiro RL, Duquette JG, Roses DF, Nunes I, Harris MN, Kamino H, et al. Induction of primary cutaneous melanocytic neoplasms in urokinase-type plasminogen activator (uPA)-deficient and

- wild-type mice: cellular blue nevi invade but do not progress to malignant melanoma in uPA-deficient animals. *Cancer Res.* 1996; 56:3597–604. [PubMed: 8758932]
15. Sabapathy KT, Pepper MS, Kiefer F, Mohle-Steinlein U, Tacchini-Cottier F, Fetka I, et al. Polyoma middle T-induced vascular tumor formation: the role of the plasminogen activator/plasmin system. *J Cell Biol.* 1997; 137:953–63. [PubMed: 9151696]
 16. Praus M, Collen D, Gerard RD. Both u-PA inhibition and vitronectin binding by plasminogen activator inhibitor 1 regulate HT1080 fibro-sarcoma cell metastasis. *Int J Cancer.* 2002; 102:584–91. [PubMed: 12447999]
 17. Soff GA, Sanderowitz J, Gately S, Verrusio E, Weiss I, Brem S, et al. Expression of plasminogen activator inhibitor type 1 by human prostate carcinoma cells inhibits primary tumor growth, tumor-associated angiogenesis, and metastasis to lung and liver in an athymic mouse model. *J Clin Invest.* 1995; 96:2593–600. [PubMed: 8675623]
 18. Gorlatova NV, Cale JM, Elokda H, Li D, Fan K, Warnock M, et al. Mechanism of inactivation of plasminogen activator inhibitor-1 by a small molecule inhibitor. *J Biol Chem.* 2007; 282:9288–96. [PubMed: 17276980]
 19. Fang H, Placencio VR, DeClerck YA. Protumorigenic activity of plasminogen activator inhibitor-1 through an antiapoptotic function. *J Natl Cancer Inst.* 2012; 104:1470–84. [PubMed: 22984202]
 20. Leik CE, Su EJ, Nambi P, Crandall DL, Lawrence DA. Effect of pharmacologic plasminogen activator inhibitor-1 inhibition on cell motility and tumor angiogenesis. *J Thromb Haemost.* 2006; 4:2710–5. [PubMed: 17010152]
 21. Miyake M, Goodison S, Giacoia EG, Rizwani W, Ross S, Rosser CJ. Influencing factors on the NMP-22 urine assay: an experimental model. *BMC Urol.* 2012; 12:23–27. [PubMed: 22928931]
 22. Anai S, Goodison S, Shiverick K, Hirao Y, Brown BD, Rosser CJ. Knock-down of Bcl-2 by antisense oligodeoxynucleotides induces radiosensitization and inhibition of angiogenesis in human PC-3 prostate tumor xenografts. *Mol Cancer Ther.* 2007; 6:101–11. [PubMed: 17237270]
 23. Badiga AV, Chetty C, Kesanakurti D, Are D, Gujrati M, Klopfenstein JD, et al. MMP-2 siRNA inhibits radiation-enhanced invasiveness in glioma cells. *PLoS ONE.* 2011; 6:e20614. [PubMed: 21698233]
 24. Pfaffl MW. A new mathematical model for relative quantification in real-time RT-PCR. *Nucleic Acids Res.* 2001; 29:e45. [PubMed: 11328886]
 25. Anai S, Sakamoto N, Sakai Y, Tanaka M, Porvasnik S, Urbanek C, et al. Dual targeting of Bcl-2 and VEGF: a potential strategy to improve therapy for prostate cancer. *Urol Oncol.* 2011; 29:421–9. [PubMed: 19576799]
 26. Rømer MU, Kirkebjerg Due A, Knud Larsen J, Hofland KF, Christensen IJ, Buhl-Jensen P, et al. Indication of a role of plasminogen activator inhibitor type I in protecting murine fibrosarcoma cells against apoptosis. *Thromb Haemost.* 2005; 94:859–66. [PubMed: 16270643]
 27. Buchholz M, Biebl A, Neesse A, Wagner M, Iwamura T, Leder G, et al. SERPINE2 (protease nexin I) promotes extracellular matrix production and local invasion of pancreatic tumors *in vivo*. *Cancer Res.* 2003; 63:4945–51. [PubMed: 12941819]
 28. Al-Fakhri N, Chavakis T, Schmidt-Woll T, Huang B, Cherian SM, Bobryshev YV, et al. Induction of apoptosis in vascular cells by plasminogen activator inhibitor-1 and high molecular weight kininogen correlates with their anti-adhesive properties. *J Biol Chem.* 2003; 384:423–35.
 29. Chen SC, Henry DO, Reczek PR, Wong MK. Plasminogen activator inhibitor-1 inhibits prostate tumor growth through endothelial apoptosis. *Mol Cancer Ther.* 2008; 7:1227–36. [PubMed: 18483310]
 30. Chorostowska-Wynimko J, Swiercz R, Skrzypczak-Jankun E, Selman SH, Jankun J. Plasminogen activator inhibitor type-1 mutants regulate angiogenesis of human umbilical and lung vascular endothelial cells. *Oncol Rep.* 2004; 12:1155–62. [PubMed: 15547731]
 31. Brooks TD, Wang SW, Brunner N, Charlton PA. XR5967, a novel modulator of plasminogen activator inhibitor-1 activity, suppresses tumor cell invasion and angiogenesis *in vitro*. *Anticancer Drugs.* 2004; 15:37–44. [PubMed: 15090742]
 32. Wiman B, Collen D. Purification and characterization of human anti-plasmin, the fast-acting plasmin inhibitor in plasma. *Eur J Biochem.* 1977; 78:19–26. [PubMed: 21075]

33. Stefansson S, Haudenschild CC, Lawrence DA. Beyond fibrinolysis: the role of plasminogen activator inhibitor-1 and vitronectin in vascular wound healing. *Trends Cardiovasc Med.* 1998; 8:175–80. [PubMed: 21235930]
34. Wilkins-Port CE, Ye Q, Mazurkiewicz JE, Higgins PJ. TGF-beta1 + EGF-initiated invasive potential in transformed human keratinocytes is coupled to a plasmin/MMP-10/MMP-1-dependent collagen remodeling axis: role for PAI-1. *Cancer Res.* 2009; 69:4081–91. [PubMed: 19383899]
35. Hennen JK, Elokda H, Leal M, Ji A, Friedrichs GS, Morgan GA, et al. Evaluation of PAI-039 [1-benzyl-5-[4-(trifluoromethoxy)phenyl]-1H-indol-3-yl](oxo)acetic acid], a novel plasminogen activator inhibitor-1 inhibitor, in a canine model of coronary artery thrombosis. *J Pharmacol Exp Ther.* 2005; 314:710–6. [PubMed: 15860572]
36. Kunz C, Pebler S, Otte J, von der Ahe D. Differential regulation of plasminogen activator and inhibitor gene transcription by the tumor suppressor p53. *Nucleic Acids Res.* 1995; 23:3710–7. [PubMed: 7479001]
37. Cooper MJ, Haluschak JJ, Johnson D, Schwartz S, Morrison LJ, Lippa M, et al. p53 mutations in bladder carcinoma cell lines. *Oncol Res.* 1994; 6:569–79. [PubMed: 7787250]
38. Mu XC, Staiano-Coico L, Higgins PJ. Increased transcription and modified growth state-dependent expression of the plasminogen activator inhibitor type-1 gene characterize the senescent phenotype in human diploid fibroblasts. *J Cell Physiol.* 1998; 174:90–8. [PubMed: 9397159]
39. Ma D, Gerard RD, Li XY, Alizadeh H, Niederkorn JY. Inhibition of metastasis of intraocular melanomas by adenovirus-mediated gene transfer of plasminogen activator inhibitor type 1 (PAI-1) in an athymic mouse model. *Blood.* 1997; 90:2738–46. [PubMed: 9326241]
40. Jankun J, Keck RW, Skrzypczak-Jankun E, Swiercz R. Inhibitors of urokinase reduce size of prostate cancer xenografts in severe combined immunodeficient mice. *Cancer Res.* 1997; 57:559–63. [PubMed: 9044824]
41. McMahon GA, Petitclerc E, Stefansson S, Smith E, Wong MK, Westrick RJ, et al. Plasminogen activator inhibitor-1 regulates tumor growth and angiogenesis. *J Biol Chem.* 2001; 276:33964–8. [PubMed: 11441025]
42. Bajou K, Maillard C, Jost M, Lijnen RH, Gils A, Declercq P, et al. Host-derived plasminogen activator inhibitor-1 (PAI-1) concentration is critical for *in vivo* tumoral angiogenesis and growth. *Oncogene.* 2004; 23:6986–90. [PubMed: 15286708]
43. Kwaan HC, Wang J, Svoboda K, Declercq PJ. Plasminogen activator inhibitor 1 may promote tumour growth through inhibition of apoptosis. *Br J Cancer.* 2000; 82:1702–8. [PubMed: 10817507]
44. Lademann U, Rømer MU, Jensen PB, Hofland KF, Larsen L, Christensen IJ, et al. Malignant transformation of wild-type but not plasminogen activator inhibitor-1 gene-deficient fibroblasts decreases cellular sensitivity to chemotherapy-mediated apoptosis. *Eur J Cancer.* 2005; 41:1095–100. [PubMed: 15862760]
45. Ramachandra M, Atencio I, Rahman A, Vaillancourt M, Zou A, Avanzini J, et al. Restoration of transforming growth factor Beta signaling by functional expression of smad4 induces anoikis. *Cancer Res.* 2002; 62:6045–51. [PubMed: 12414627]
46. Schneider DJ, Chen Y, Sobel BE. The effect of plasminogen activator inhibitor type 1 on apoptosis. *Thromb Haemost.* 2008; 100:1037–40. [PubMed: 19132227]
47. Bajou K, Peng H, Laug WE, Maillard C, Noel A, Foidart JM, et al. Plasminogen activator inhibitor-1 protects endothelial cells from FasL-mediated apoptosis. *Cancer Cell.* 2008; 14:324–34. [PubMed: 18835034]
48. McGarvey TW, Kariko K, Barnathan ES, Thomas J, Malkowicz SB. The expression of urokinase-related genes in superficial and invasive transitional cell carcinoma. *Int J Oncol.* 1998; 12:175–80. [PubMed: 9454902]
49. Kobayashi H, Fujishiro S, Terao T. Impact of urokinase-type plasminogen activator and its inhibitor type 1 on prognosis in cervical cancer of the uterus. *Cancer Res.* 1994; 54:6539–48. [PubMed: 7987854]
50. Tee YT, Wang PH, Tsai HT, Lin LY, Lin HT, Yang SF, et al. Genetic polymorphism of urokinase-type plasminogen activator is interacting with plasminogen activator inhibitor-1 to raise risk of cervical neoplasia. *J Surg Oncol.* 2012; 106:204–8. [PubMed: 22354580]

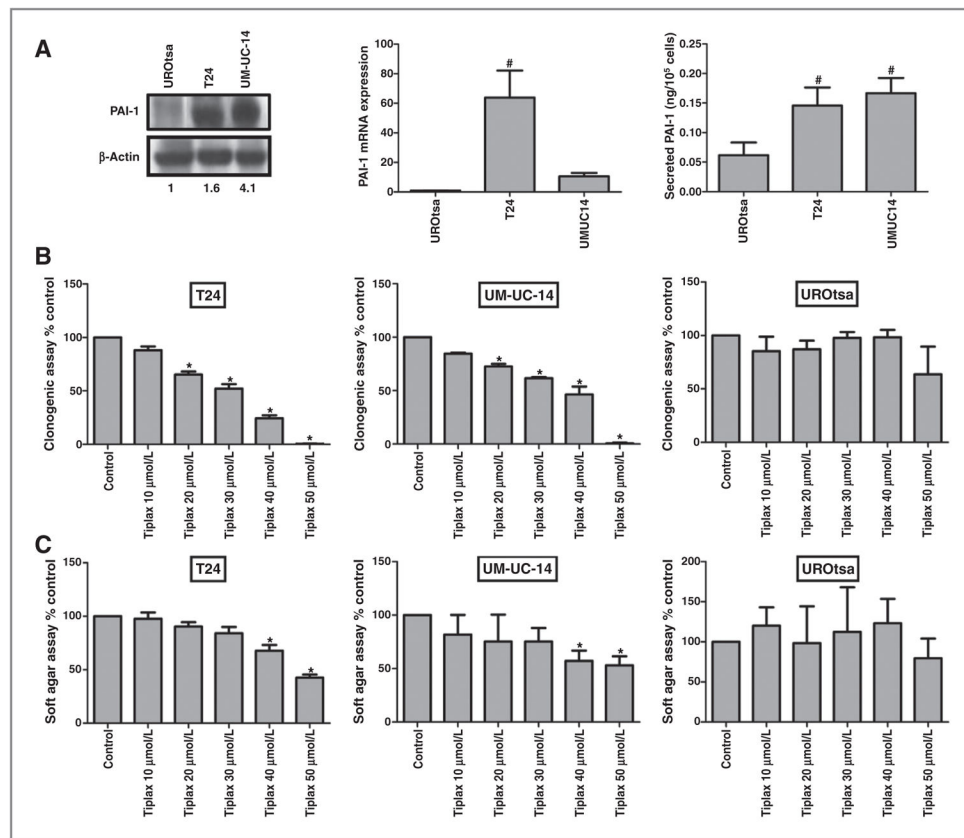
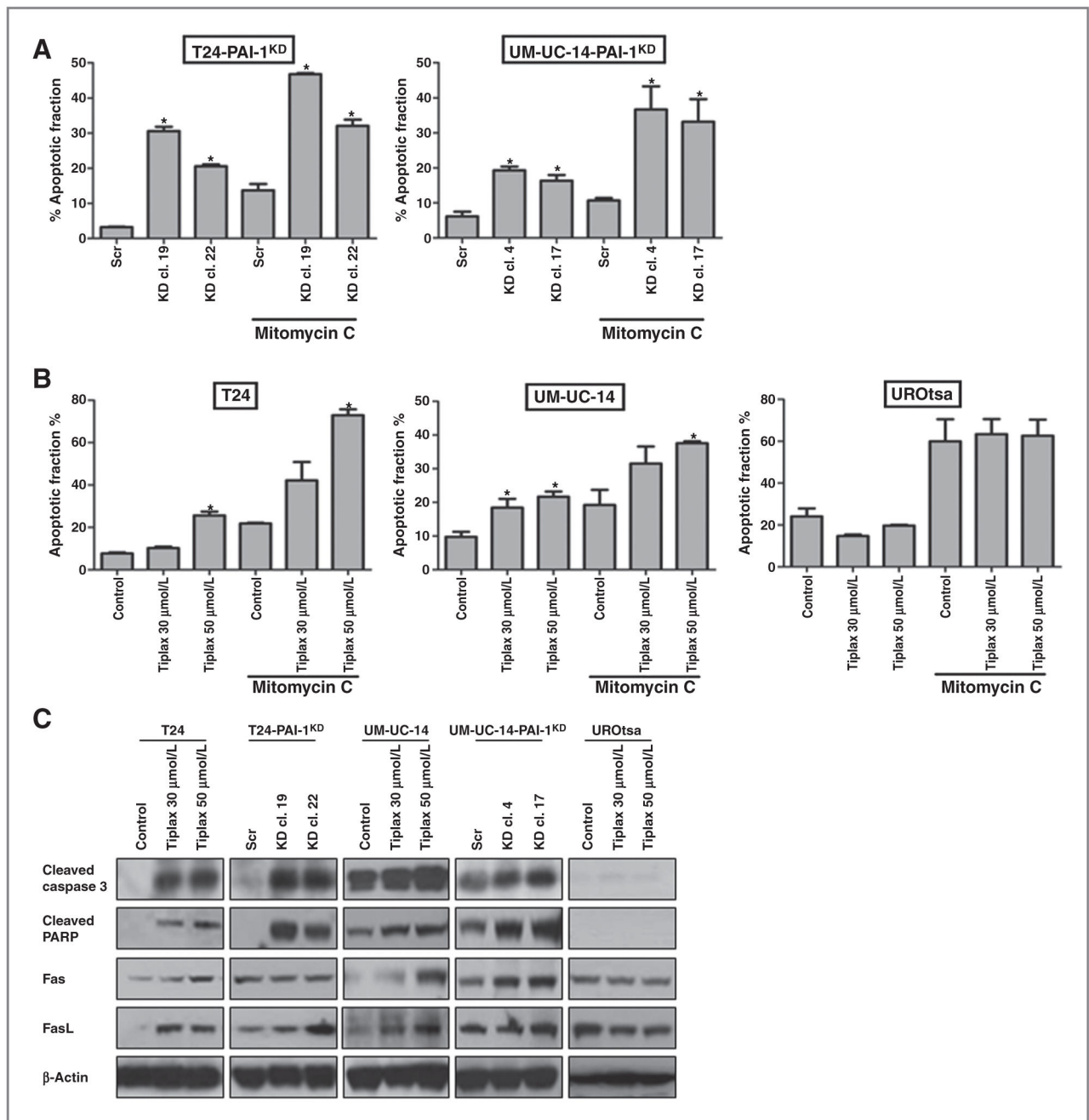
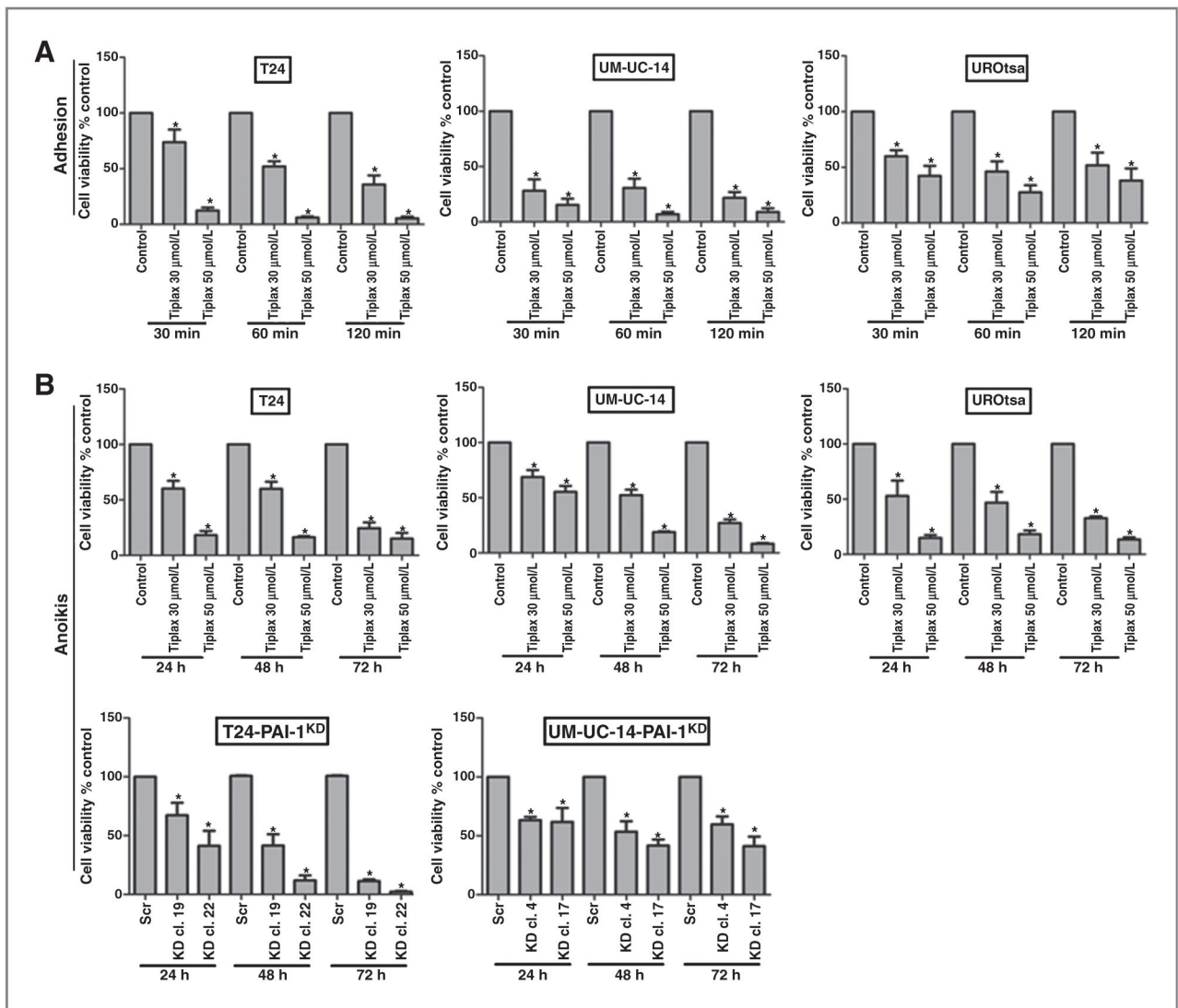


Figure 1. Effect of PAI-1 small-molecule inhibitor on proliferation and colony formation in human urothelial cell lines. A, PAI-1 levels were evaluated in UROtsa, T24, and UM-UC-14 cells by immunoblotting, densitometry of immunoblot, quantitative PCR, and ELISA. Analysis of human urothelial cell lines confirmed upregulation of PAI-1 protein in T24 and UM-UC-14 urothelial cancer cells but not in UROtsa benign bladder cells. Numbers below Western blot analysis image lanes are from semiquantitative densitometric analysis. B, about 10^3 urothelial cells were seeded in 6-well plates exposed to tiplaxtinin at the indicated concentration for 72 hours followed by aspiration of culture media and replacement with fresh complete media. Cells were incubated for an additional 14 days. After 14 days, colonies were fixed with 6.0% glutaraldehyde, stained with 0.5% crystal violet, and counted under light microscopy. Data were represented as the mean \pm SD of three independent replicates. C, about 2×10^3 urothelial cells pretreated with tiplaxtinin at the indicated concentration were mixed in agar solution and fresh complete media and seeded in 96-well plates. Cells were incubated for 6 to 8 days. Colony formation was quantified using the fluorescent cell stain CyQUANT GR Dye (Cell Biolabs Inc.) in the FLUOstar OPTIMA Reader. Data were represented as mean \pm SD of three independent replicates. All experiments were repeated at least three times. Targeting PAI-1 was noted to retard cellular proliferation and colony formation. *, $P < 0.05$.

**Figure 2.**

Silencing of PAI-1 results in induction of apoptosis. A, annexin V apoptotic assay was performed in the T24 clones (T24-PAI-1^{KD}-19, T24-PAI-1^{KD}-22 compared with T24^{Scr}) and UM-UC-14 clones (UM-UC-14-PAI-1^{KD}-4, UM-UC-14-PAI-1^{KD}-17 compared with UM-UC-14^{Scr}) after exposing the cells to the apoptotic-inducing agent, mitomycin C at 5 $\mu\text{g}/\text{mL}$. The antiapoptotic effects of PAI-1 overexpression were abrogated in T24 clones (T24-PAI-1^{KD}-19 and T24-PAI-1^{KD}-22), UM-UC-14 clones (UM-UC-14-PAI-1^{KD}-4 and UM-UC-14^{KD}-17). B, annexin V apoptotic assay was also performed in parental T24, UM-UC-14, and UROtsa cells treated with and without tiplaxtinin (30 and 50 $\mu\text{mol/L}$) and

exposed to the apoptotic inducing agent, mitomycin C at 5 $\mu\text{g}/\text{mL}$. C, Western blot analysis was performed on the above cell lines confirming the induction of the key apoptotic proteins cleaved caspase-3, cleaved-PARP, Fas, and FasL. Staining for β -actin served as a control. At least three independent experiments consisting of each condition tested in triplicate wells was used to calculate mean \pm SD values. *, $P < 0.05$.

**Figure 3.**

Targeting PAI-1 results in a reduction in adhesion and increased rates of anoikis. A, in a cell adhesion assay, treatment of T24, UM-UC-14, and UROtsa cells with 30 and 50 $\mu\text{mol/L}$ tiplaxtinin resulted in a dose-dependent reduction in the ability of the cells to adhere to substrate. B, in an anoikis assay, treatment of T24, UM-UC-14, and UROtsa cells with 30 and 50 $\mu\text{mol/L}$ tiplaxtinin for 24 hours resulted in significant induction of anoikis. Furthermore, genetic knockdown of PAI-1 also resulted in increased rates of anoikis of T24 clones and UM-UC-14 clones.

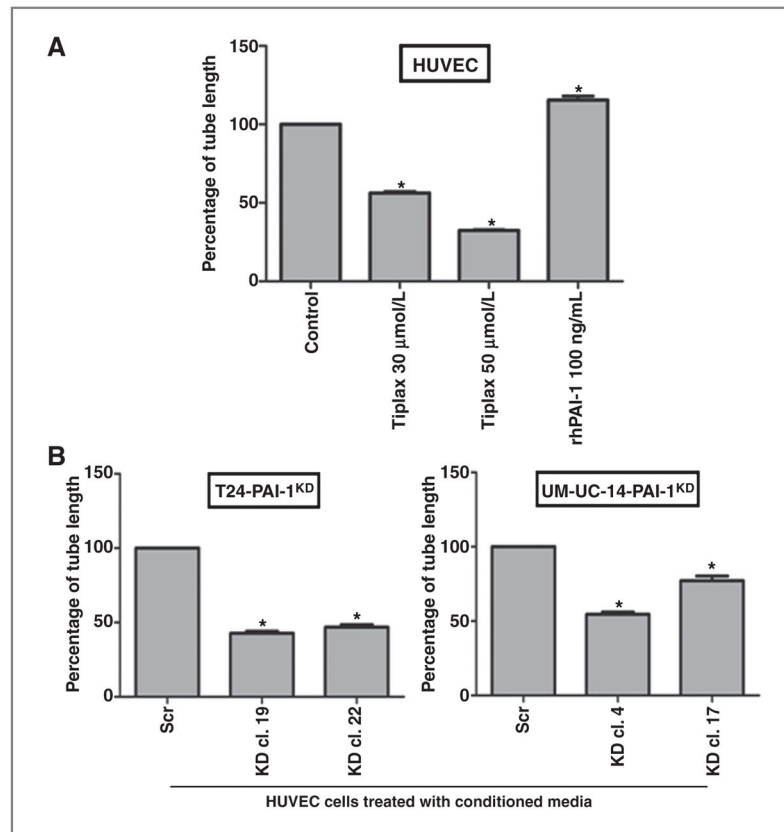


Figure 4.

Knockdown of PAI-1 influenced endothelial tube formation. A, capillary tube formation in HUVECs cultured in growth factor-rich Matrigel with tiplaxtinin and/or rhPAI-1 was quantified as total tube length. Although rhPAI-1 enhanced stimulation of tube formation, tiplaxtinin significantly diminished the proangiogenic effects of PAI-1. B, capillary tube formation in HUVECs cultured in conditioned media from T24 clones (T24-PAI-1^{KD}-19 and T24-PAI-1^{KD}-22 compared with T24^{Scr}) and UM-UC-14 clones (UM-UC-14-PAI-1^{KD}-19 and UM-UC-14-PAI-1^{KD}-22 compared with UM-UC-14^{Scr}) was quantified as total tube length per well in micrometer. Reduction in PAI-1 expression in T24-PAI-1^{KD} and UM-UC-14-PAI-1^{KD} clones was associated with a significant reduction in tube formation in HUVEC cells. Data from representative experiments are presented as mean \pm SD. All experiments were repeated at least three times. *, $P < 0.05$.

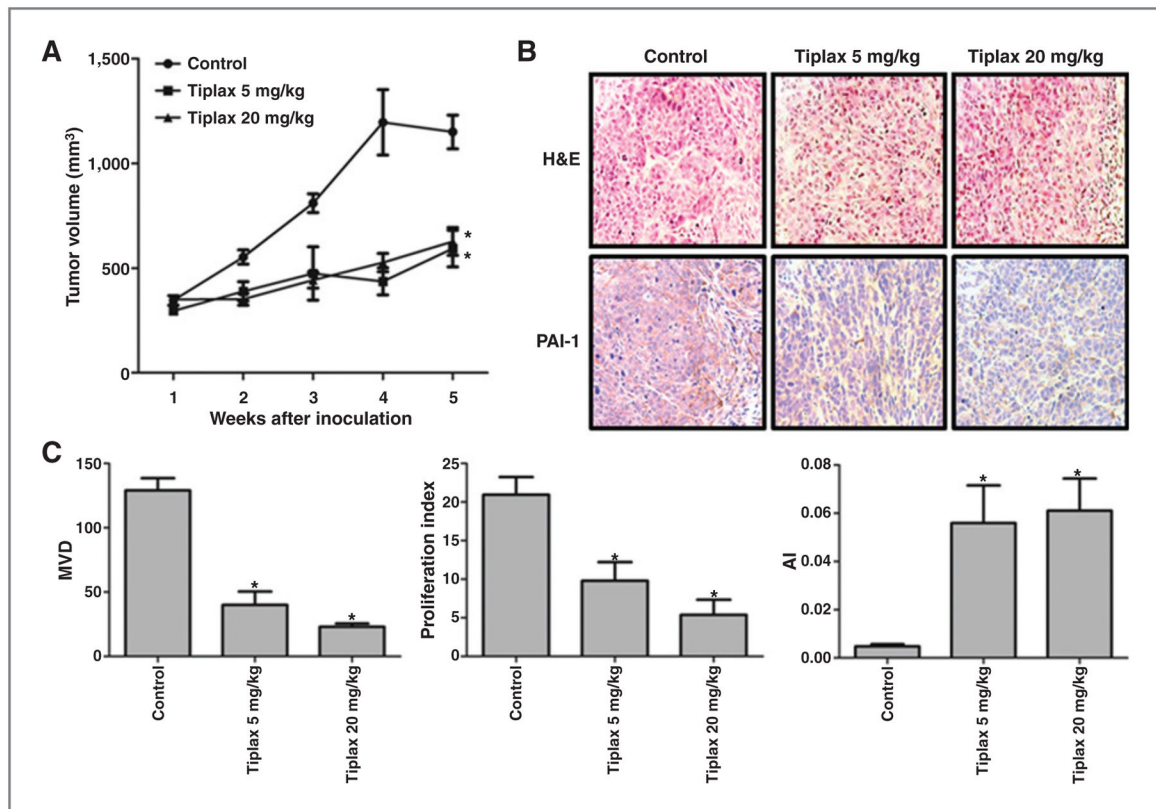


Figure 5.

Effect of targeting PAI-1 in a T24 bladder cancer xenograft tumor model. Tumor growth was established by subcutaneous injection of parental T24 cells into athymic nude mice (nu/nu) followed by the oral administration of tiplaxtinin at two different doses as described in Materials and Methods. Corn oil administered orally served as control. A, T24 tumor sizes were recorded over 5 weeks. The relative tumor size was plotted as mean \pm SD from the three treatment groups per cell line ($n = 10$ per group). Treatment with tiplaxtinin (5 mg/kg and 20 mg/kg) was associated with a reduction in T24 tumor burden. B, H & E and PAI-1 staining of T24 tumors are shown (images $\times 200$). A reduction in PAI-1 expression was noted in T24 tumors treated with tiplaxtinin. C, MVD was quantified on the basis of CD31 staining as previously reported (22). Proliferative index was quantified on the basis of Ki-67 staining as previously reported (22). Apoptotic index (AI) was quantified on the basis of cleaved caspase-3 staining as previously reported (22). Tiplaxtinin treatment of T24 xenografts was associated with a reduction in angiogenesis and proliferation with an accompanied induction of apoptosis. Data from one representative experiment are presented as the mean \pm SD. *, $P < 0.05$.